

An Experimental Approach to the Nature  
and Characteristics of Primary Fission Fragments ✓

Peter C. Stevenson and Harry G. Hicks

Lawrence Radiation Laboratory, University of California,  
Livermore, California

December 1964

*(Received 5 February 1965)*

ABSTRACT

Positive ions of charges 1, 2, 3, and 4 were obtained for each of several masses in a beam of recoiling fission fragments from a thick  $U^{235}$  target. The existence of such low-charged ions was demonstrated by resolving the beam after passing it through parallel electric and magnetic fields. Energies of these low-charged ions are approximately proportional to their charges. Abundances of the low-charged ions are of the order of 1/2% of the total number of emitted fission fragments. At higher charges, the charge on a fission fragment emitted from a thick source appears to be roughly proportional to its velocity.

Abundances of low-charged ions appear to depend on their chemical properties.

INTRODUCTION

Although a great deal of precise experimental information is now available concerning the distribution of mass between the two fragments of a fissioning nucleus, the analogous problem of the distribution of nuclear charge in fission is in a much less satisfactory state. If in the "act of fission" we include the emission of the prompt neutrons, the mass of each fission product is established (except for the rare case of the delayed neutron emitters) as

soon as fission is complete, and the study of fission yield as a function of mass can be carried out at a rate well suited to radiochemical or mass-spectrometric techniques. This is not true of nuclear charge; the vast majority of fission fragments undergo several changes of nuclear charge via beta decay before being transformed into species sufficiently long-lived for radiochemical or mass-spectrometric study.

Some information is available; Wahl et al.<sup>1</sup> have measured direct fission yields of two or three isobaric nuclides in each of several mass chains that are susceptible to rapid chemical separation. The technique is unfortunately, limited to regions with amenable chemistry and to species with half-lives of a few seconds or more. Cohen and Fulmer<sup>2</sup> have made an ingenious application of the mass-spectrometric technique to the study of the charge distribution of fission fragments escaping from a thin source into low-pressure gas. From the observed relationship between mass resolution and gas pressure, they were able to deduce a "width" of the charge distribution curve for the mass 97 fission product chain of about 2.2 charge units. It is unfortunate that their method has an optimum mass resolution of several mass numbers.

The study of the nuclear charge distribution of a large number of fission product mass chains demands a rapid separation of species. Such a separation need not isolate one single nuclide, although that would be the ideal case; it is enough to separate a small group of nuclides that can be measured in the presence of each other by suitable methods. Previous investigators have usually isolated a group of isotopes of a single element by chemical methods. An equally good method, permitting even simpler resolution, would be to isolate the isobars of a single mass number; for example, by passage through a mass spectrometer. In either case the amount of each species present in the mixture is determined by resolving the multicomponent decay curves, by

differential counting, by chemical separation of daughter products, or by some other appropriate method. We shall consider here a method based on the separation of a group of isobars.

The average number of beta decays associated with a given fission fragment is about three or four.<sup>3</sup> Assuming that fission products more than eight beta decays away from stability are not formed in appreciable yield, one predicts half-lives of the order of 0.1 second or greater for the primary products, using a semi-empirical mass equation such as that of Levy<sup>4</sup> with standard beta-decay theory. Thus the time from scission to complete passage through a mass spectrometer can be kept short enough so that no appreciable beta decay will occur.

Since all mass separations operate on the ratio of mass to ionic charge, ambiguities in observed mass can result unless the fission fragments have a defined ionic charge, e. g., a mass-to-charge ratio of 25 could result from unresolved masses of 75, 100, 125, and 150 with charges of 3, 4, 5, and 6 respectively. Only species of a single charge give mass to charge ratios that are unambiguous over nearly the entire mass range (Fig. 1). Lassen<sup>5</sup> has shown that the ionic charges on fission fragments originating in a thin source range from 16 to 28; one would therefore expect considerable ambiguity in the interpretation of most charge-to-mass ratios. Some of this ambiguity could be resolved by constructing a high-resolution machine; however, it seems advisable either to search for a means of reducing the spread in the values of the ionic charges, or to attempt to develop a system having at least an appreciable abundance of singly-charged species.

The second alternative seems more reasonable to attempt, since we assume that interaction with matter will reduce the charge as well as the energy

of a moving fragment, but no simple approach seems available to reduce the charge spread of the original fragments. One would therefore like to design a system such that exactly the right amount of matter could be interposed between the fission source and the mass-separation device to reduce the most likely charge on each fragment to unity. The appropriate amount of matter is presumably a function of fission fragment mass number, nuclear charge, and original kinetic energy; since these factors all vary widely, the selection of an "appropriate amount" is extremely difficult. The problem can be very simply avoided by using the fissionable material itself as the absorber; if one uses a source of fissionable material that is thicker than one range of fission fragments, there will always be some appropriate depth within the source that will be covered with the proper amount of matter such that any given species will have maximum probability of emerging from the surface with a single charge. Fragments originating at a greater depth will emerge uncharged, or fail to emerge; those originating at a lesser depth will emerge with charges greater than one. The question of the intensity of the singly-charged fragment beam from such a thick source remains to be determined; for proper design of an apparatus for mass separation we also require information about the energy spectrum of such a beam.

The feasibility of this experimental approach, then, depends 1) on the intensity of the singly-charged fission fragment beam emergent from a thick piece of fissionable material immersed in an available neutron flux, and 2) on the ability to design and build a device for separating such fragments. Determination of the abundance and approximate energy spectrum of the singly-charged fission fragment beam emergent from a thick source constitutes the experimental part of this report.

## EXPERIMENTAL

The best practical instrument to use in a study of ion source characteristics is the parallel-field analyzer originally developed by Thomson.<sup>6</sup> In this device, the beam of ions is passed through parallel electric and magnetic fields, these fields being transverse to the original direction of the beam, as indicated in Fig. 2. After leaving the region of the fields, the beam travels a certain distance and impinges on a plate perpendicular to the original beam direction. A system of rectangular coordinates may be set up on such a plate with the origin at the point of impact of the undeflected beam, the x axis in the direction in which the beam is displaced by the electric field, and the y axis in the direction in which the beam is displaced by the magnetic field.

The equations of motion of an ion in the arrangement of fields shown in Fig. 2 can be solved exactly, but are quite complicated. However, in the case where the radius  $a$  of the circular magnetic field is much less than the radius of curvature  $R$  of the ion trajectory in the magnetic field, a relatively simple approximate solution can be obtained. These equations can then be used to give initial conditions of motion of the ion in the field-free space between the deflecting system and the collector plate. They in turn permit evaluation of the deflections  $x$  (by the electric field) and  $y$  (by the magnetic field) of the point of impact of the ion beam, as functions of the velocity  $v$ , mass  $m$ , and charge  $q$  of the ions, the electric and magnetic field strengths  $E$  and  $H$ , and the dimensions of the apparatus ( $a$  and  $l$  in Fig. 2);

$$y \cong \frac{2 a l H}{c} \cdot \frac{1}{v} \cdot \frac{q}{m} \quad (1)$$

$$x \cong a l E \cdot \frac{2}{v^2} \cdot \frac{q}{m} = a l E \cdot \frac{q}{1/2 m v^2} \quad (2)$$

( $c$  is the velocity of light).

$v$  can be eliminated between Eqs. (1) and (2) to give

$$x \cong \frac{1}{2 a \ell} \cdot \frac{E c^2}{H^2} \cdot \frac{m}{q} \cdot y^2 \quad (3)$$

From Eq. (3) we see that all particles of a particular  $m/q$  will strike the plate somewhere along a parabolic locus which is characteristic of that  $m/q$  ratio. From Eq. (2) we see that the particular point struck by a given particle is a measure of the ratio of charge to kinetic energy of that particle.

The apparatus shown in Fig. 3 was designed for use in conjunction with the Livermore Pool-Type Reactor (LPTR) at the Lawrence Radiation Laboratory in Livermore. A 0.001-inch-thick foil of  $U^{235}$  was mounted on an aluminum plug and inserted into an evacuated tube in a hole in the reactor shielding. The thermal neutron flux at the inner end of the hole was approximately  $5 \times 10^{12}$  neutrons/cm<sup>2</sup>/second. The beam of fragments passed along the tube, through a collimating hole furnished with a remotely-controlled shutter, and between the poles of a 12-inch-diameter electromagnet. Also between the poles of the magnet were a pair of parallel plates, one at ground potential, the other insulated and connected to a source of negative high voltage (up to 20 kV). The beam entered the field region close to the grounded plate to avoid edge effects insofar as possible. On emerging from the field region, the beam travelled for about 1 meter and impinged on a piece of 0.001-inch-thick aluminum foil fastened to a rigid backing. Pressure in the entire system was kept below  $10^{-6}$  torr.

The uranium foil was inserted in the beam tube with the reactor shut down, the tube was evacuated, and the reactor started. When full reactor power was reached (2 MW) the magnet and high voltage were turned on and the

beam shutter opened. Fission fragments were allowed to accumulate on the collector foil for periods ranging from a day to a week. The reactor was then shut down, and the collector foil was immediately removed, placed in contact with a large x-ray film, and left for a period ranging between 8 and 48 hours.

A sketch representing a typical autoradiograph of the collector foil is shown in Fig. 4; although the contrast was low in the original autoradiograph, it was possible to see bands of radioactivity. Positions of these bands, in order of appearance from the right of the picture, correspond to the heavy group of fission fragments, charge 1; the light group, charge 1; the heavy group, charge 2; the heavy group, charge 3; and the light group, charge 2, superimposed; the heavy group, charge 4; and the light group, charge 3, superimposed; and others not clearly resolved. The great majority of the beam, as might have been expected, lies in the large region at the left of the picture, containing ions of higher charge. (The original autoradiograph could not be reproduced for publication due to poor contrast.)

A certain amount of information is available from inspection of the pattern. First, ions of low charge do indeed occur in appreciable abundance. Second, the energy range for low-charged ions is broad but limited, the range being about a factor of 2. Third, the charge on a slowly-moving fission fragment is approximately proportional to its energy, since the electrical displacement of the bands for ions of low charge is roughly constant. Finally the charge on an energetic ion is approximately proportional to its velocity, since the magnetic deflections of the highly-charged ions do not vary as much as might be expected.

Following the autoradiographic examination, the collector foils were cut apart and the pieces analyzed separately for various fission products. The method of cutting depended on a simple geometric property of the parabola.

For a parabola described by the equation  $x = ky^2$ , a line passing from a point  $(x_1, y_1)$  on the parabola through a point  $(-x_1, 0)$  on the x axis is tangent to the parabola at the point  $(x_1, y_1)$ , (Fig. 5). In the region of interest, the parabolic arcs can be approximated reasonably well by straight lines. The collector foil was cut (Fig. 6) into a series of pieces of equal area. The method of cutting accepts particles of energies between 1 and 3 MeV per unit charge. These pieces were dissolved separately and analyzed radiochemically for a variety of fission products. The total remaining area of the foil in the quadrant where activity is expected was also analyzed to give a measure of the total beam intensity. A measure of background level was obtained by analysis of that part of the foil lying in the other quadrants.

From Eq. (3) above,  $y^2 = k \cdot \frac{q}{m} \cdot x$ ; from the method of cutting,  $x$  is taken as constant. On analyzing for a product of a particular mass, we only expect to find activity for integral values of  $q$ . It is convenient, therefore, to plot a graph of counts per minute as ordinate against  $y^2$  as abscissa, with  $y$  measured to the center of the trapezoidal section. We expect to find equally spaced maxima, the difference in abscissa between maxima corresponding to a change of  $q$  of one electronic charge. The spacing between the ordinate axis and the first maximum should be the same as the spacing between adjacent peaks if the first maximum does indeed represent a singly-charged species.

Figure 7 represents results obtained by counting the total gamma radiation emitted by sections of the collector foil cut as for analysis. The predicted positions of the various species are indicated on the figure, H and L standing respectively for "heavy group" and "light group," and the number representing ionic charge. There is a general background level which is probably due to fission-product activity thermally evaporated from the source; however,

peaks are clearly defined. The overall fraction of typical singly-charged fragments seems to be between 0.1% and 0.2% of the total beam for both the light and the heavy groups of fragments.

Figures 8 through 15 present the results of several experiments in which radiochemical analyses were made for a number of nuclides. The principal difficulty encountered was due to the large amount of fission-produced heat liberated in the source. The resulting elevated temperature frequently induced recrystallization of the enriched uranium fission source foil, which apparently resulted in the release of large quantities of volatile fission products. These products passed down the beam tube as gases and the daughters were deposited on the collector foil. Fission products with rare gas precursors spread over the entire collection foil obscuring the position of those fragments of the same mass separated by the spectrometer. The  $Ba^{140}$  data (Fig. 8) are presented to illustrate the difficulty.

Subsequently, the apparatus was modified to permit the insertion of a thin film, penetrable by energetic fission fragments but not by diffusing gas, at a point in the beam tube prior to the collimator. The thin film did not survive long (1 week) irradiations and was replaced by a wire grid biased to -90 V about 1 cm from the collector foil to collect daughters of radioactive gaseous fission fragments. The collector foil was grounded. The wire was 0.002 inch in diameter and passed over the collector foil at 1 cm intervals. This screen reduced general background levels to acceptable values. Unfortunately, the  $Ba^{140}$  was not remeasured with the screen in place; however, the  $Sr^{91}$  data were taken with the screen in place and provide a sharp contrast to those of  $Ba^{140}$  without the screen.

There is clear indication in many cases of the resolution of low charged species (+1 to +4). Repetition of the  $Zr^{97}$  and  $Mo^{99}$  data (Figs. 10, 11) with

differing magnetic field intensities gave the same fraction of the total beam in the +1 charge state.

Table I presents the results of a series of runs on seven different masses. The fraction of the total beam present in each ionic charge state is given for each mass measured. It is obvious that the charge pattern varies strongly from mass to mass. In an attempt to understand the reason for the behavior of each mass chain, we have also tabulated the composition of each mass chain at the time of formation as calculated by Weaver et al.<sup>7</sup> The lower part of Table I is arranged so that the elements making up the lower-mass chains (91, 97, and 99) are on the same row of the table as the homologous elements making up the higher-mass chains (131, 132, 141, and 143). While the prediction of chain composition cannot be regarded as reliable in the present state of knowledge of the fission process, it should serve as a general guide.

Some correlation of charge distribution with chemical properties is at once apparent. Masses 97 and 99, with similar precursors, have similar charge distribution patterns; so also do masses 131 and 132. Mass 91, for which the most abundant species is a noble gas, has a high abundance of single and double charges; mass 143 has a low abundance of the noble-gas member of the chain and a much lower abundance of single-charge beam than of double-charge; mass 141 has a substantially higher abundance of noble gas and a higher abundance of single charges.

While the data are sparse and the predictions of chemical nature uncertain, there are enough indications of dependence of charge distribution on chemical nature to be quite interesting. At the same time, such a dependence makes the experimental measurement of independent isobaric yields by study of the low-charged fragments considerably more difficult than was anticipated.

It seems appropriate to consider whether any possible chemical effect may contribute to the discrepancy between mass spectrometric methods of chain-length measurement as exemplified by the work of Armbruster et al.<sup>8</sup> and other methods of deducing chain length as given for example in the paper of Wahl et al.<sup>1</sup> or the papers of Glendenin et al.<sup>9</sup> and Bowman.<sup>10</sup> The discrepancy appears to be serious enough to indicate that a real phenomenon other than experimental error may be involved, although at very high ion energies chemical effects would seem to be unlikely a priori.

The single-charge parabola for mass 99 has been examined in detail by sectioning it into pieces corresponding to 0.25 MeV energy intervals. The energy spectrum of the mass-99 singly-charged ions is shown in Fig. 16. The energy appears to be quite sharply peaked at about 1.6 MeV, and nearly all the beam is included in the energy region between 1.25 and 2.25 MeV.

### CONCLUSIONS

The existence of singly-charged fission fragments emerging from a thick source of fissionable material has been conclusively demonstrated. The abundance of such fragments is small relative to that of the fragments of higher charge; however, with a suitably high flux one could presumably obtain a high enough intensity for investigation, depending upon the nature of the proposed experiment.

The practical problem of designing a mass-separator to work on the obtainable particle beam is severe, though not insuperable. The low abundance of singly-charged ions means that one requires either a high neutron flux or a large-area source; either alternative requires the removal of a considerable amount of heat from the source region to avoid the emission of volatile products. A more difficult problem is the design of the separator itself; the high

energy per unit charge and wide spread in the particle energy imply that a device of sufficient transmission and resolution must be quite large and must employ quite high fields, which in turn implies a large, expensive device. It also seems probable that the interpretation of the data obtained from such a machine would be complicated by a possible chemical effect on the intensity of the low-charged ion beams obtained. It seems desirable to search for another approach to the problem, reserving the possibility of designing such an apparatus as a last resort.

#### ACKNOWLEDGMENTS

The authors wish to express their appreciation to the crew of the LPTR for their aid in performing the experiments and to Mrs. Nancy Sawley and Miss Alice Conover for technical assistance in counting the samples and data reduction.

Table I. Abundance of low-charge species.

Charge:	Mass:	91	97	99	131	132	141	143
		Percent of Total Beam						
1		1.1	0.58	0.30	0.24	0.80	0.76	0.06
2		1.9	0.57	0.31	<0.1	<0.2	0.61	0.31
3		n.m	0.59	0.42	<0.1	<0.1	0.95	0.67
4		n.m	n.m	0.79	~0.1	<0.1	1.60	~1.0

Predicted Chemical Nature at Time of Formation  
(Percent of Chain)

--	--	--	--	In	6.1	1.2	--	--
--	--	--	--	Sn	33.1	21.3	--	--
--	--	--	--	Sb	44.7	48.7	--	--
Se	0.8	--	--	Te	15.7	<u>28.8</u>	--	--
Br	18.9	--	--	I	<u>0.3</u>		0.6	
Kr	46.4	--	--	Xe			18.0	3.2
Rb	29.5	--	--	Cs			46.0	25.0
Sr	<u>4.5</u>	11.1	8.2	Ba			30.0	45.9
Y		44.9	37.7	La			5.3	23.7
Zr		<u>44.0</u>	42.7	Ce			<u>0</u>	<u>2.2</u>
Nb			11.2	--				
Mo			<u>0.2</u>	--				

REFERENCES

\*Work performed under the auspices of the U. S. Atomic Energy Commission.

<sup>1</sup>A. C. Wahl, R. L. Ferguson, D. R. Nethaway, D. E. Troutner, and K. Wolfsberg, *Phys. Rev.* 126, 1112 (1962).

<sup>2</sup>B. L. Cohen and C. B. Fulmer, *Nucl. Phys.* 6, 547 (1958).

<sup>3</sup>K. Way and E. P. Wigner, in Radiochemical Studies: The Fission Products, N.E.E.S., Div. IV, P.P. R., Vol. 9, paper 43, page 436 (McGraw-Hill, New York, 1951).

<sup>4</sup>H. B. Levy, *Phys. Rev.* 106, 1265 (1957).

<sup>5</sup>N. O. Lassen, *Kgl. Danske Videnskab. Selskab, Mat Fys. Medd.* 26, Nr. 5 (1951).

<sup>6</sup>J. J. Thomson, *Phil. Mag.* 21, 225 (1911).

<sup>7</sup>L. E. Weaver, P. O. Strom, and P. A. Killeen, NRDL-TR-633 (5 March 1963).

<sup>8</sup>P. Armbruster, D. Hovestat, H. Meister, and H. J. Specht, *Nucl. Phys.* 54, 586 (1964).

<sup>9</sup>L. E. Glendenin, J. P. Unik, and H. C. Griffin, Symposium on the Physics and Chemistry of Fission, Salzburg (1965), International Atomic Energy Agency (proceedings to be published).

<sup>10</sup>H. R. Bowman, S. G. Thompson, R. L. Watson, S. S. Kapoor, and J. O. Rasmussen, Symposium on the Physics and Chemistry of Fission, Salzburg (1965), International Atomic Energy Agency (proceedings to be published).

5001843

## FIGURE CAPTIONS

Fig. 1. Yield (atoms per hundred fissions) of fission products of various masses plotted against mass-to-charge ratio of fragments for various assumed values of the ionic charge. It can be seen that only the curve for charge 1 (extreme right-hand curve in the figure) is essentially free of overlap with curves for other charges. Curves for charges higher than 4 are omitted for clarity. All such curves would lie between existing curves and the vertical axis, with a great deal of overlap on the charge 3 and 4 curves.

Fig. 2. Schematic views of the essential parts of the Thomson parallel field mass analyzer.

Fig. 3. Fission-fragment analyzer used to obtain the data in this report.

Fig. 4. Outline of autoradiograph of collector foil from fission-fragment analyzer. Circular area at right represents the undeflected beam. Dotted line indicates position of one of the coordinate axes. Magnetic deflection is horizontal (leftward), electric deflection is vertical (downward). In the original autoradiograph faint smudges representing lower-charged fission fragments could be seen to the right of the large irregular area. The ellipsoidal areas labeled HI, LI, and so on are the resolved low-charge beams. H indicates "heavy fragment"; L indicates "light fragment." The numeral next to each letter indicates the assumed fragment ionic charge.

Fig. 5. A line from the point  $(-x_1, 0)$  to the parabola at the point  $(x_1, y_1)$  is tangent to the parabola at that point. This line therefore represents an approximation to the parabola in the neighborhood of  $(x_1, y_1)$ .

Fig. 6. Method of cutting collector foil for radiochemical analysis. The trapezoidal sections are rough approximations to parabolic arcs passing through the origin and through the centers of the trapezoids.

Fig. 7. Gross activity of cut sections of collector foil, showing predicted positions of light and heavy fission fragments. The general background level is presumed to come from deposition of fission products thermally evaporated from the source. This background level persists over the entire collector foil.

Fig. 8. Low charged fragments of mass 140 as measured by  $\text{Ba}^{140}$  have been obscured by decay products from thermally evaporated  $\text{Xe}^{140}$ .

Fig. 9. Low charged fragments of mass 91 as measured by  $\text{Sr}^{91}$ .

Fig. 10. Low charged fragments of mass 97 as measured by  $\text{Zr}^{97}$ .

Fig. 11. Low charged fragments of mass 99 as measured by  $\text{Mo}^{99}$ .

Fig. 12. Low charged fragments of mass 131 as measured by  $\text{I}^{131}$ .

Fig. 13. Low charged fragments of mass 132 as measured by  $\text{Te}^{132}$ .

Fig. 14. Low charged fragments of mass 141 as measured by  $\text{Ce}^{141}$ .

Fig. 15. Low charged fragments of mass 143 as measured by  $\text{Ce}^{143}$ .

Fig. 16. Energy spectrum of singly charged mass 99 fission fragments emerging from a thick uranium source.

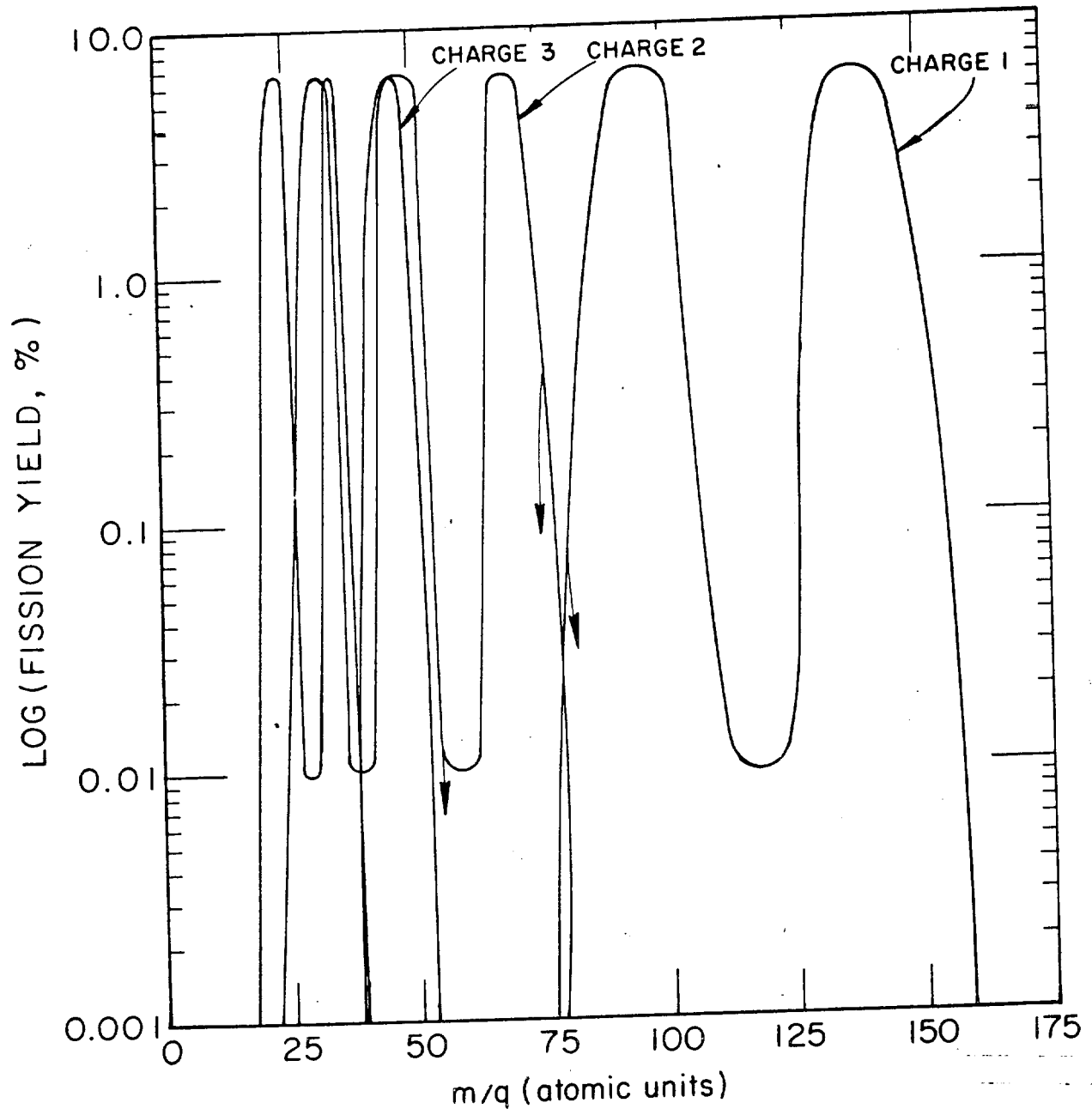
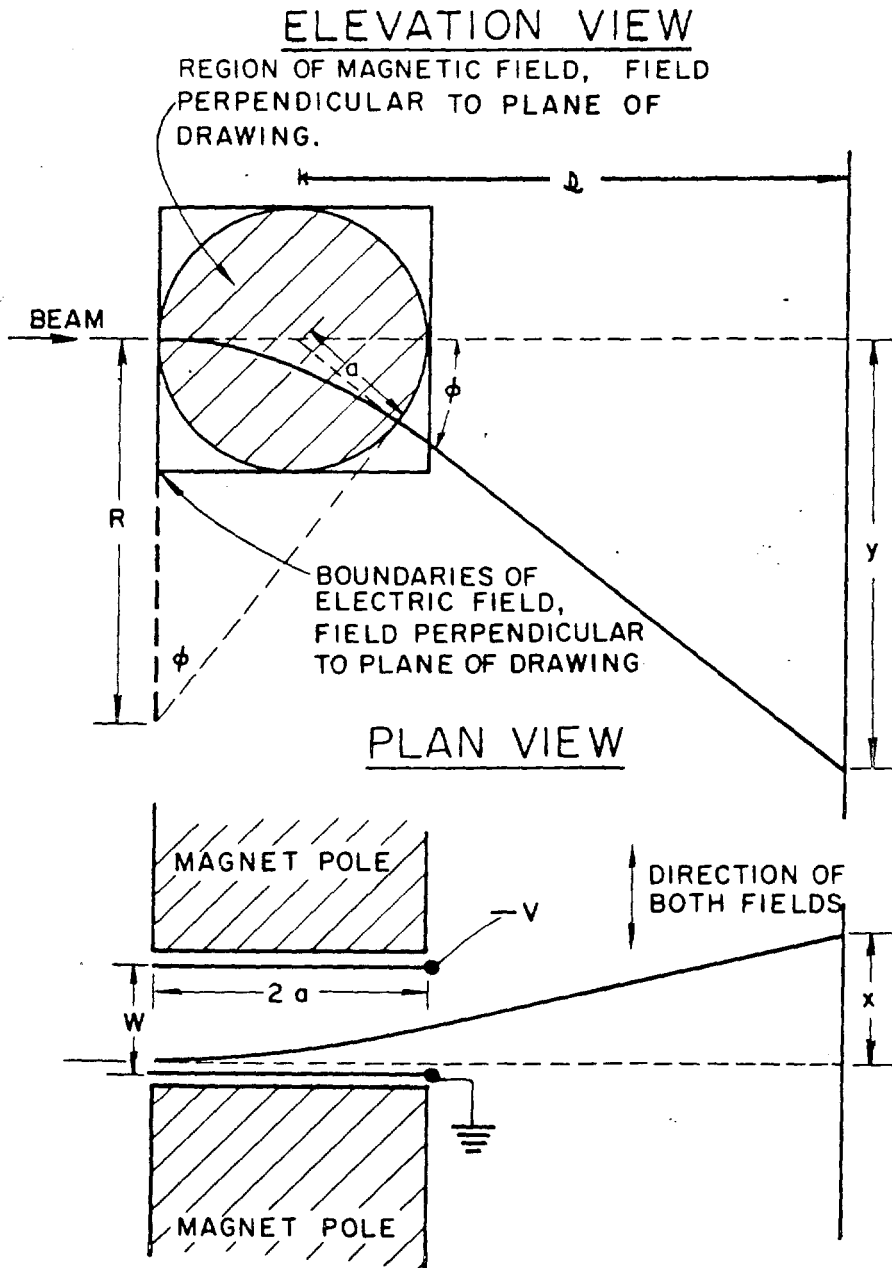


Fig. 1 - UCRL-6491 Rev. **IV**  
Authors: P.C. Stevenson and  
H.C. Hicks

5001846

42



$$\tan \phi/2 = \frac{a}{R}$$

$$\therefore \tan \phi = \frac{2aR}{R^2 - a^2}$$

$$\therefore y = \frac{2atR}{R^2 - a^2}$$

$$R = \frac{m}{q} \cdot v \cdot \frac{c}{H}$$

$$y = \frac{2at}{R [1 - (a/R)^2]}$$

$$y = \frac{2atH}{c [1 - (a/R)^2]} \cdot \frac{1}{v} \cdot \frac{q}{m}$$

$$y = \frac{2atH}{c} \cdot \frac{1}{v} \cdot \frac{q}{m}$$

since  $a/R \ll 1$

$$x \approx at \frac{v}{W} \cdot \frac{q}{1/2 mv^2}$$

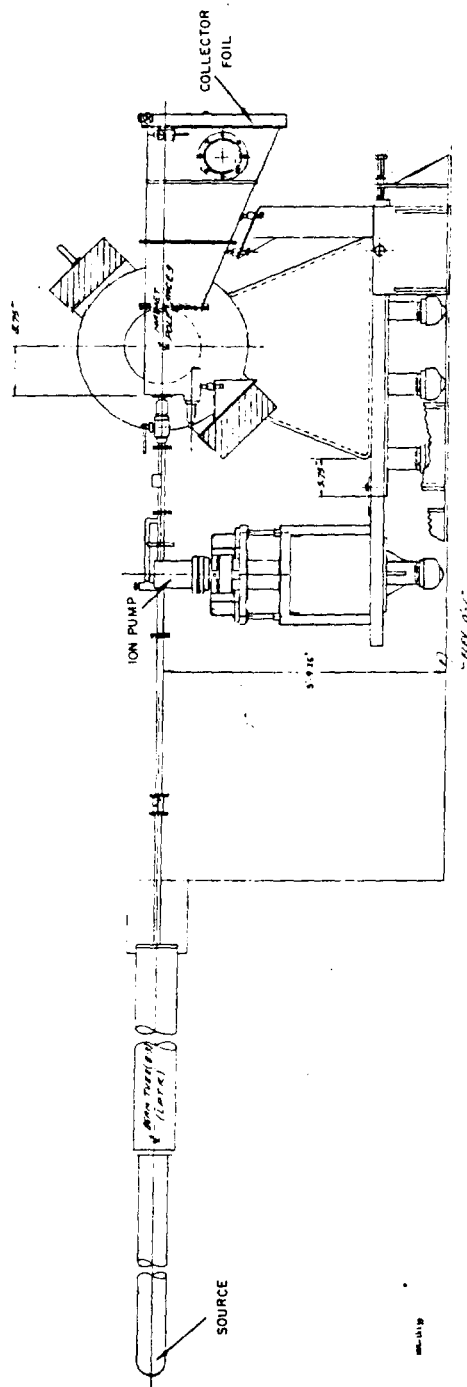
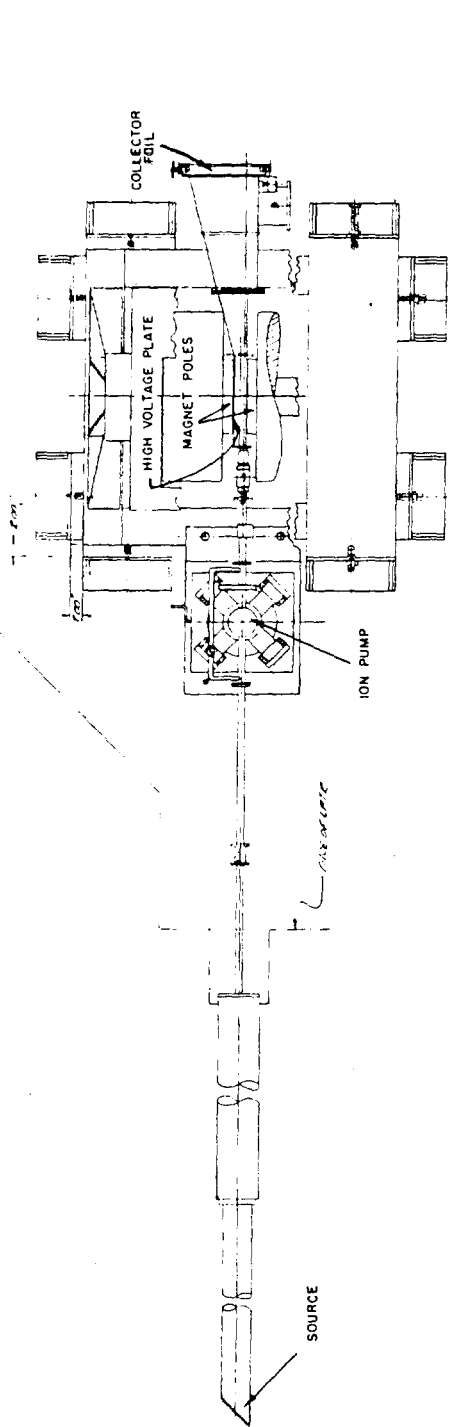
$$x \approx \frac{2atV}{W} \cdot \frac{1}{v^2} \cdot \frac{q}{m}$$

$$\therefore x \approx \frac{1}{2atW} \cdot \frac{c^2 V}{H^2} \cdot \frac{m}{q} y^2$$

5001847

Fig. 2 - UCRL-6491 Rev. IV  
 Authors: P. C. Stevenson and  
 H. C. Hicks

*PK*



5001848

Fig. 3 - UCRL-6491 Rev. II  
 Authors: P. C. Stevenson and  
 H. G. Hicks

*PH*

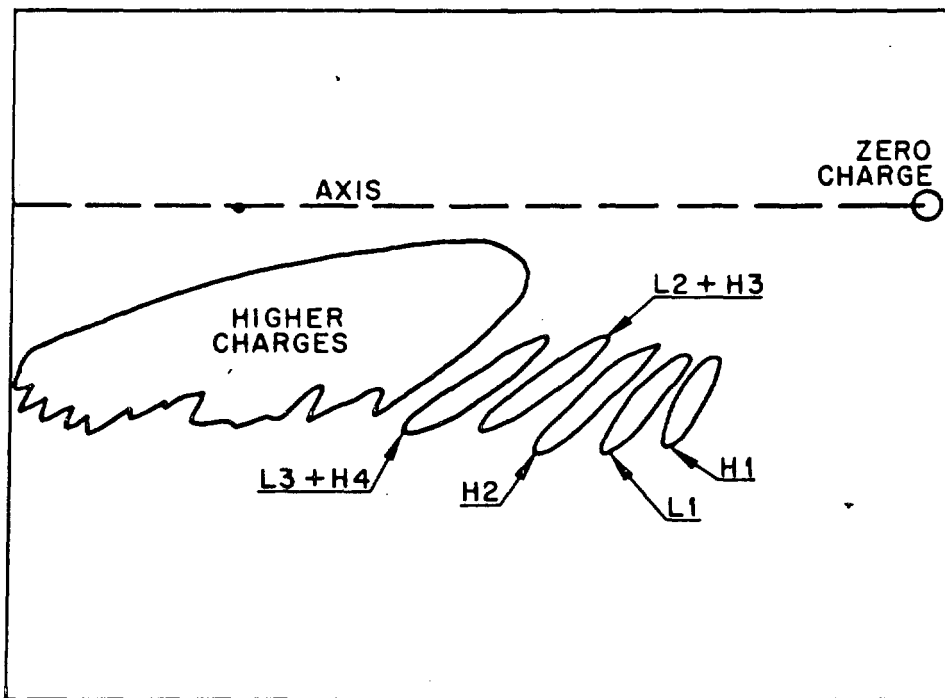
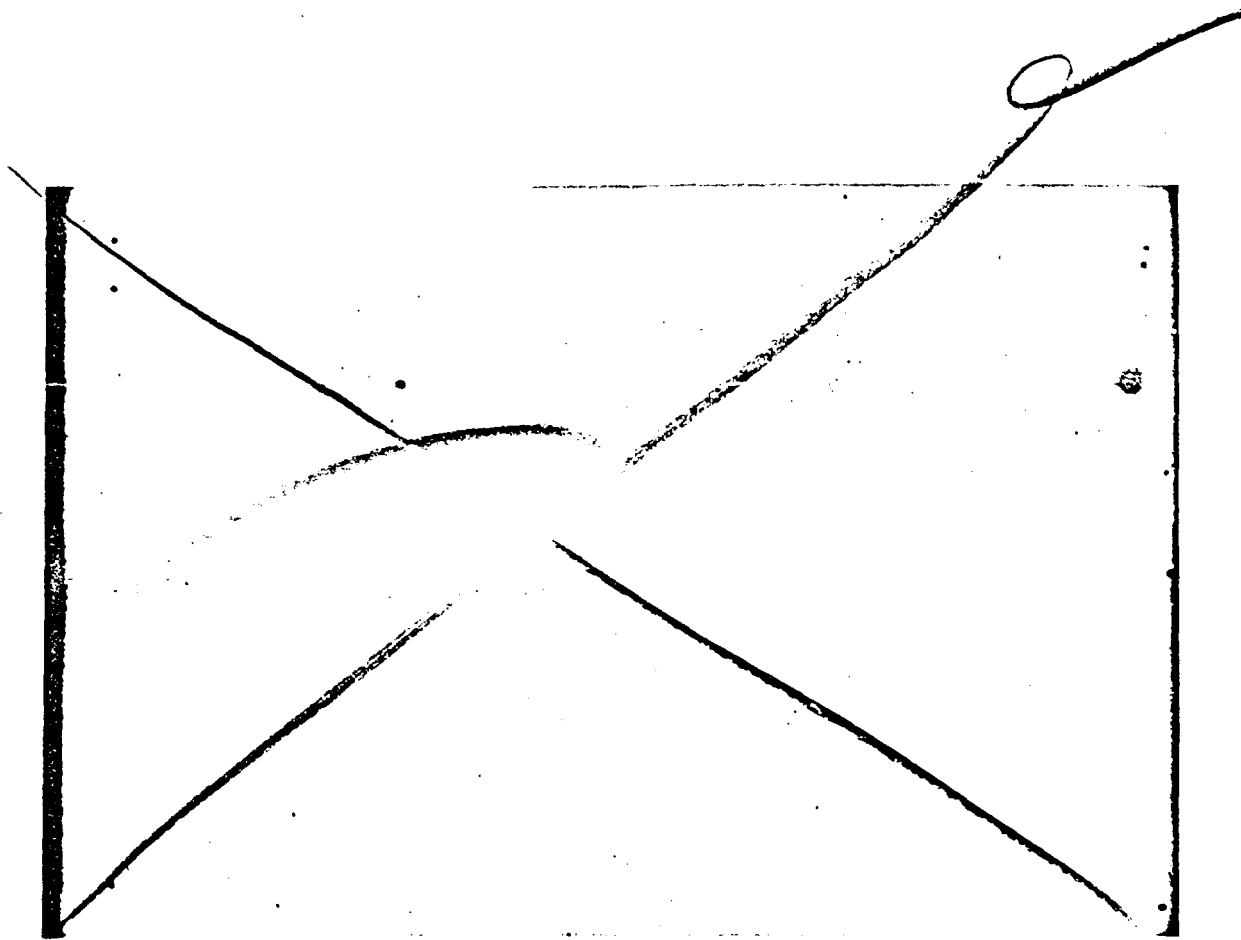


Fig. 4 - UCRL-6491 Rev. II  
 Authors: P. C. Stevenson and  
 H. C. Hicks *PH*

5001849

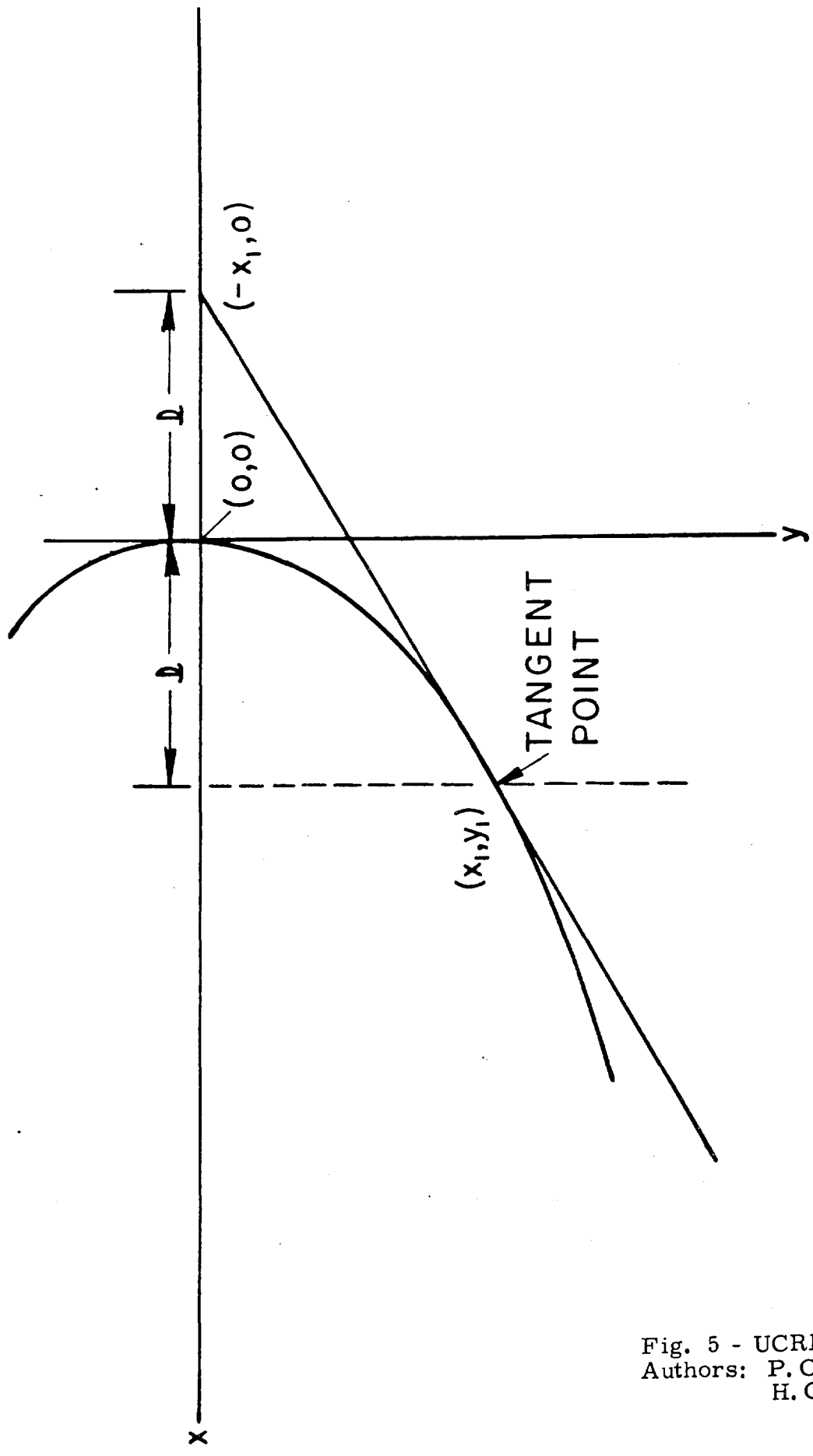


Fig. 5 - UCRL-6491 Rev. II  
 Authors: P. C. Stevenson and  
 H. C. Hicks *PH*

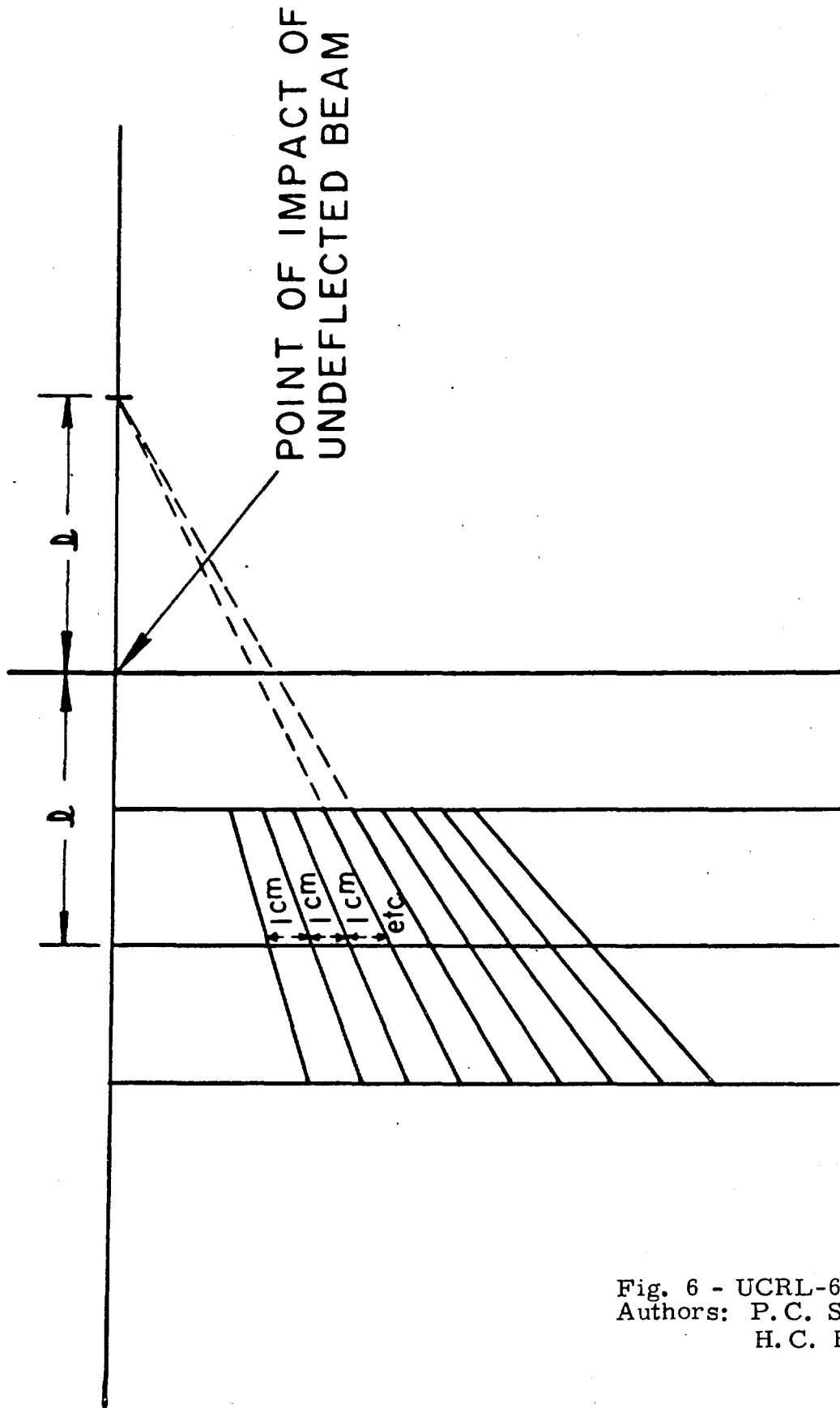


Fig. 6 - UCRL-6491 Rev. II  
 Authors: P. C. Stevenson and  
 H. C. Hicks

*PK*

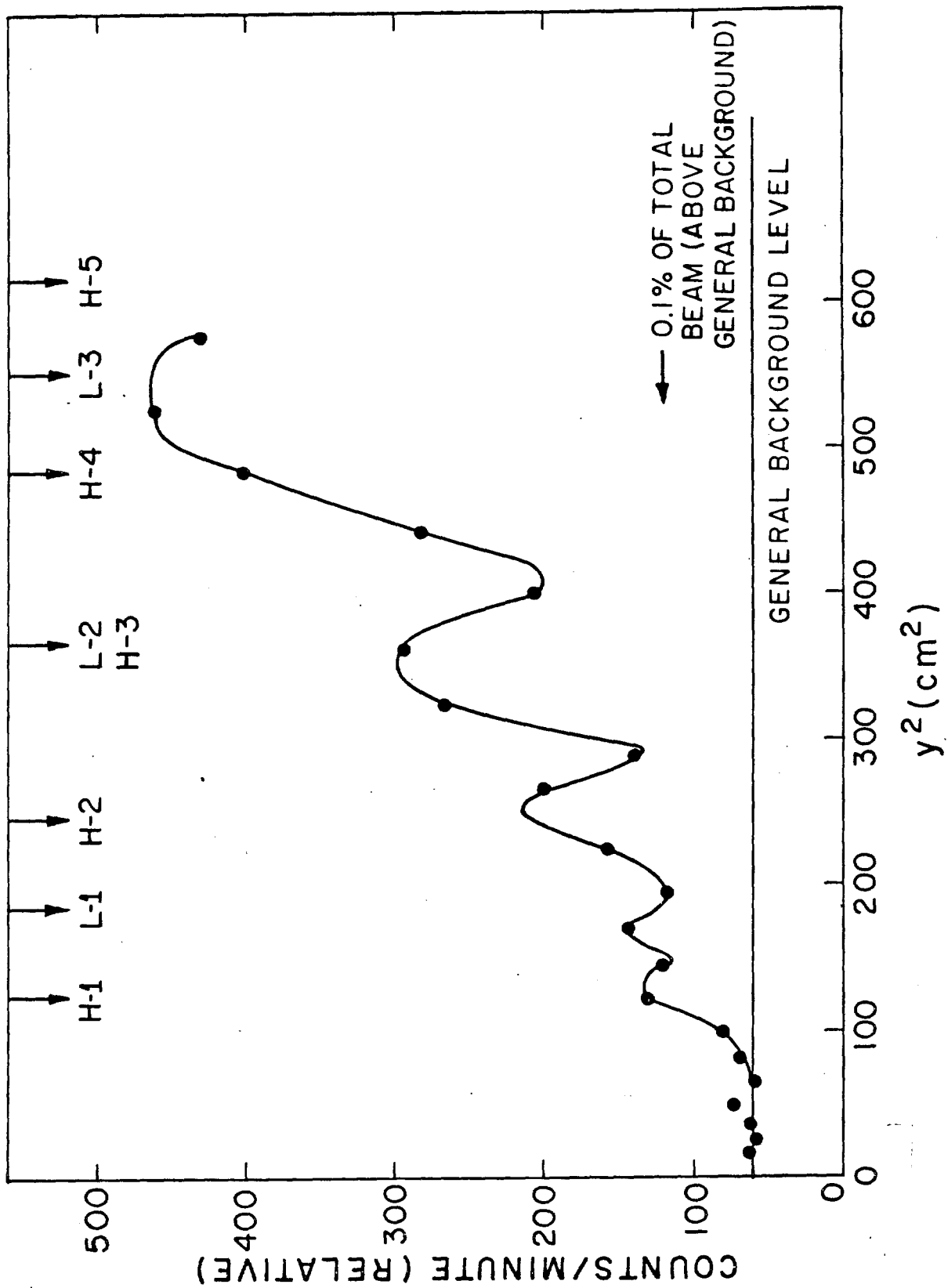


Fig. 7 - UCRL-6491 Rev. II  
 Authors: P. C. Stevenson and  
 H. C. Hicks

5001852

*PH*

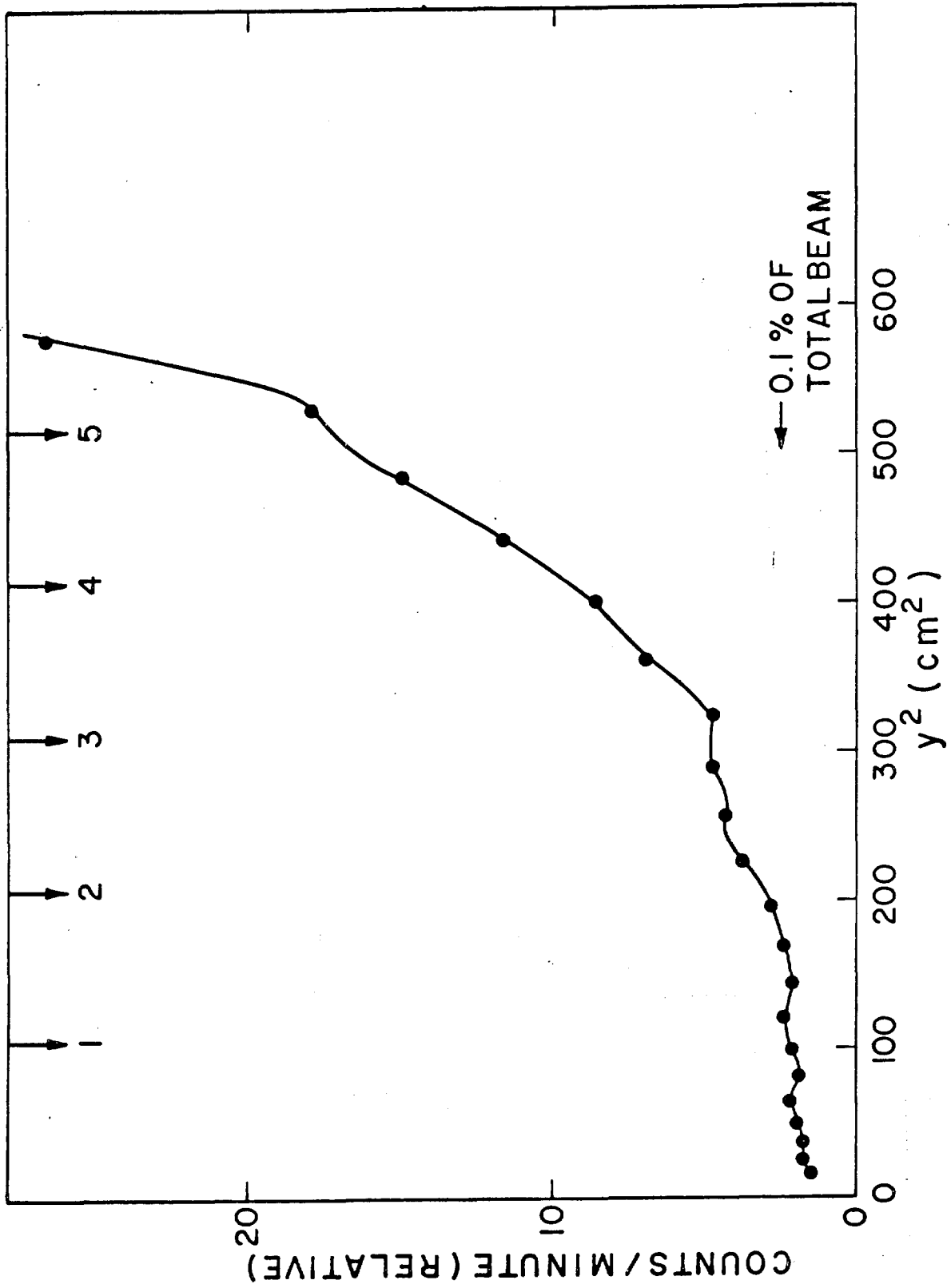


Fig. 8 - UCRL-6491 Rev. II  
 Authors: P. C. Stevenson and  
 H. C. Hicks *PH*

5001853

5001854

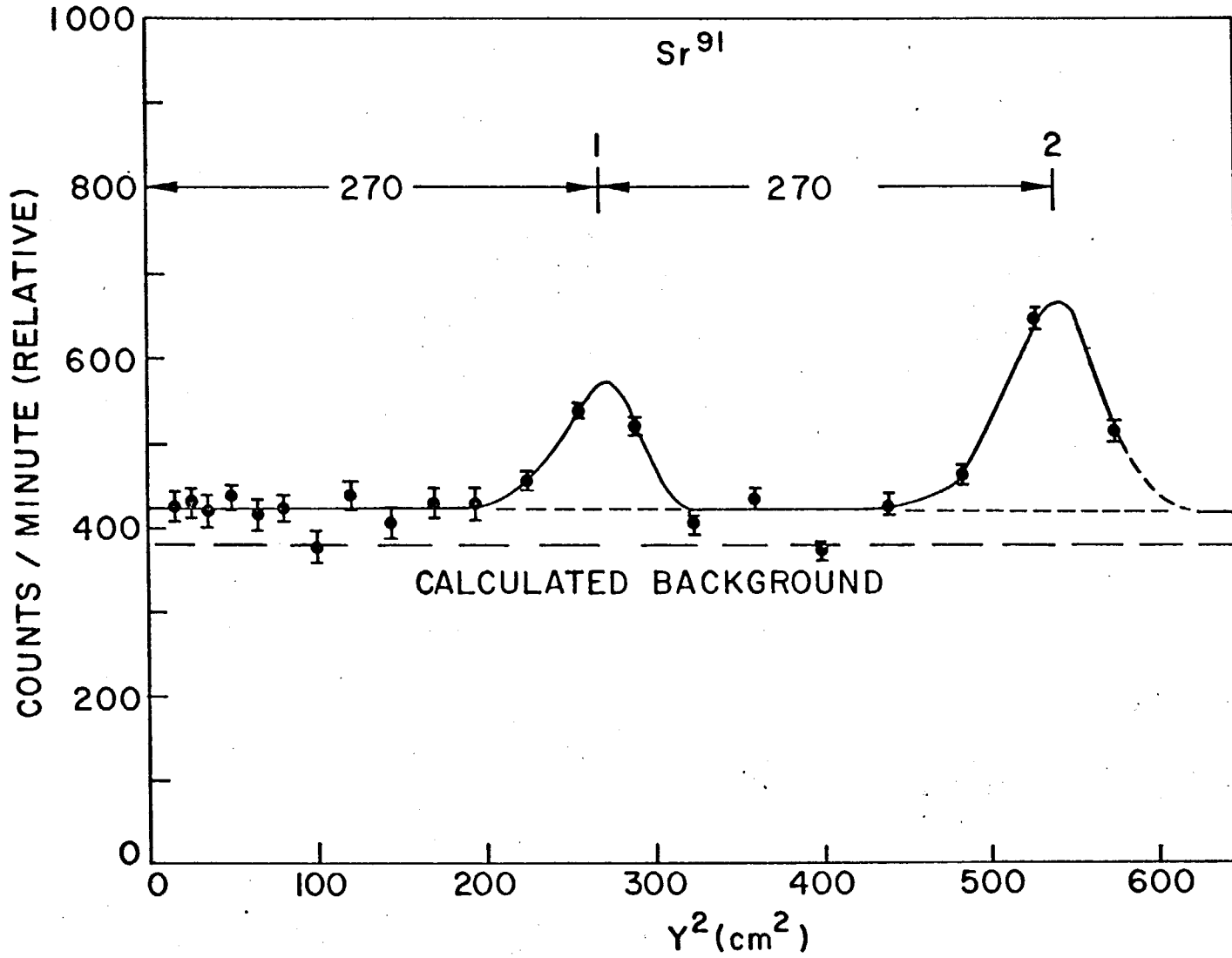


Fig. 9 - UCRL-6491 Rev. II  
Authors: P. C. Stevenson and  
H. C. Hicks  
*PK*

5001855

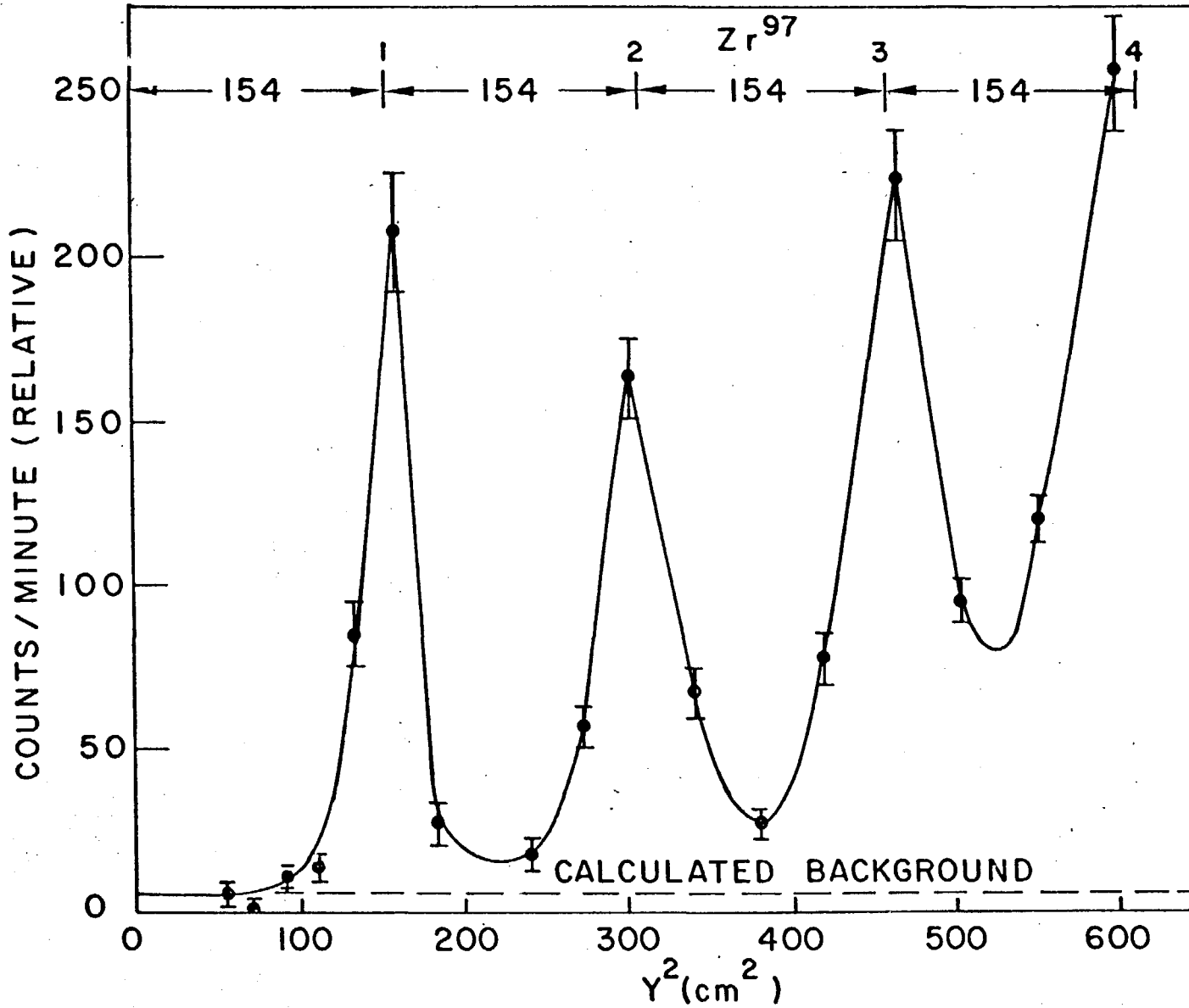


Fig. 10 - UCRL-6491 Rev. II  
Authors: P.C. Stevenson and  
H.C. Hicks

*PK*

5001856

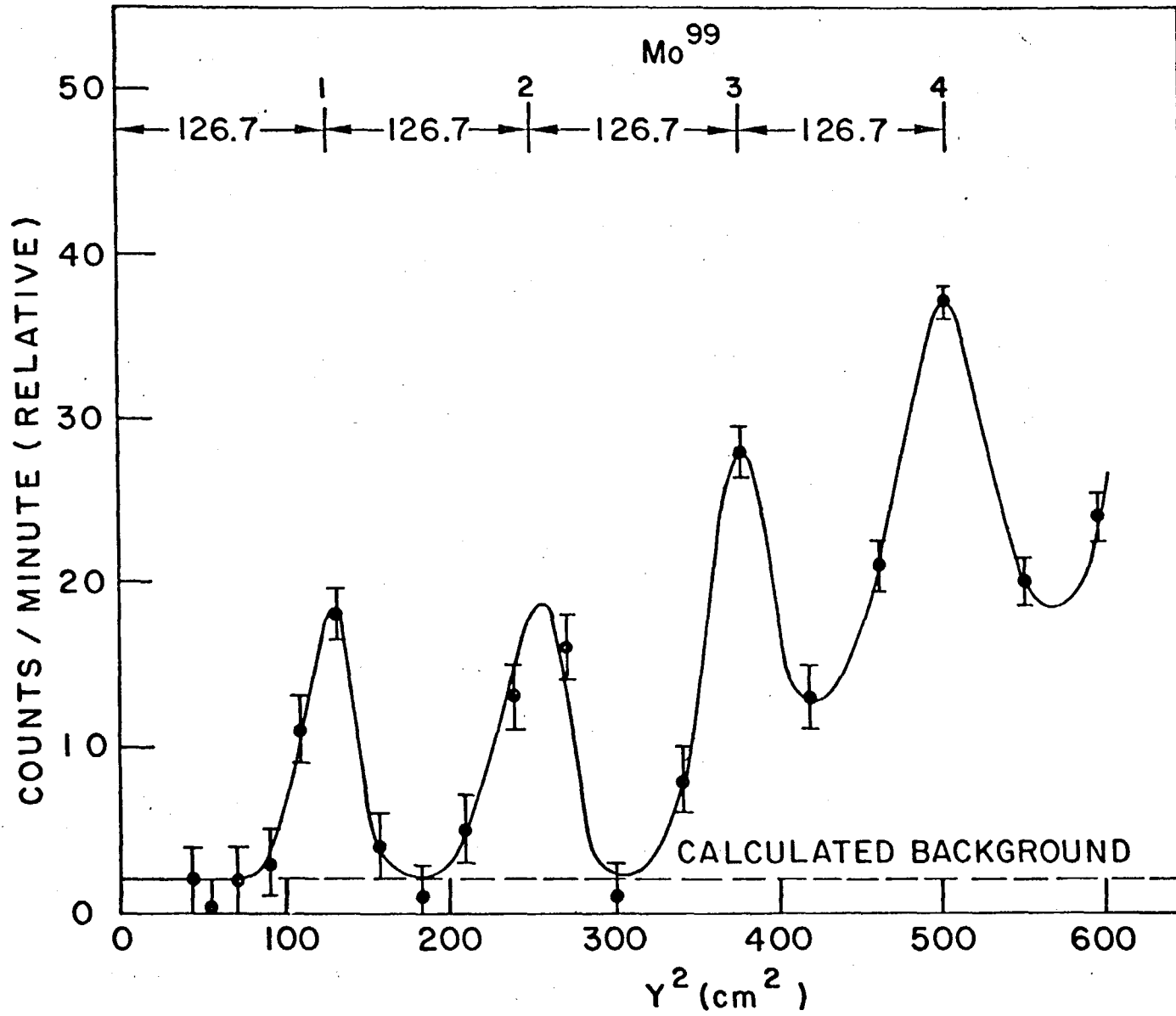


Fig. 11 - UCRL-6491 Rev. II  
Authors: P. C. Stevenson and  
H. C. Hicks

PK

5001857

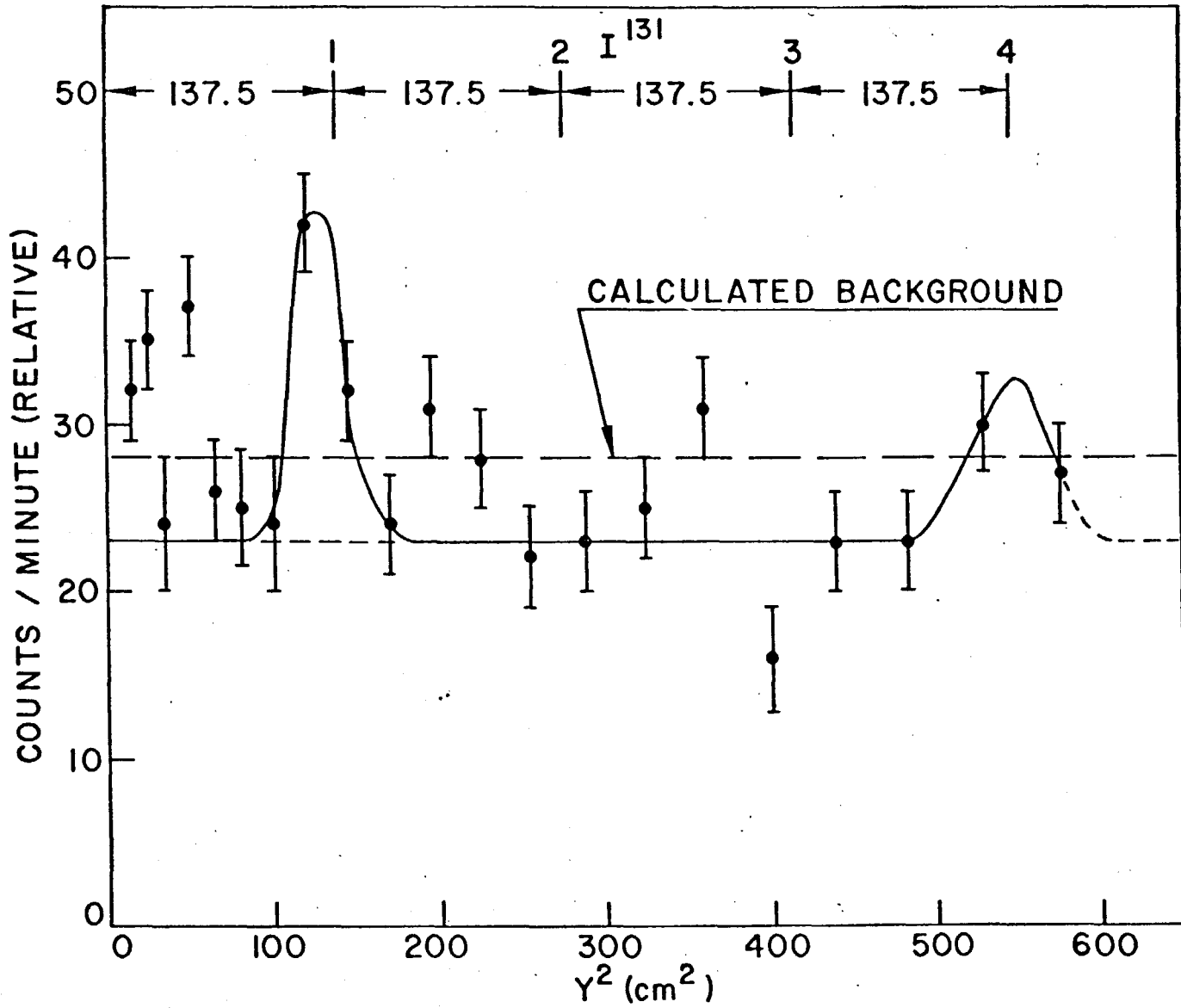


Fig. 12 - UCRL-6491 Rev. II  
Authors: P.C. Stevenson and  
H.C. Hicks

PK

5001858

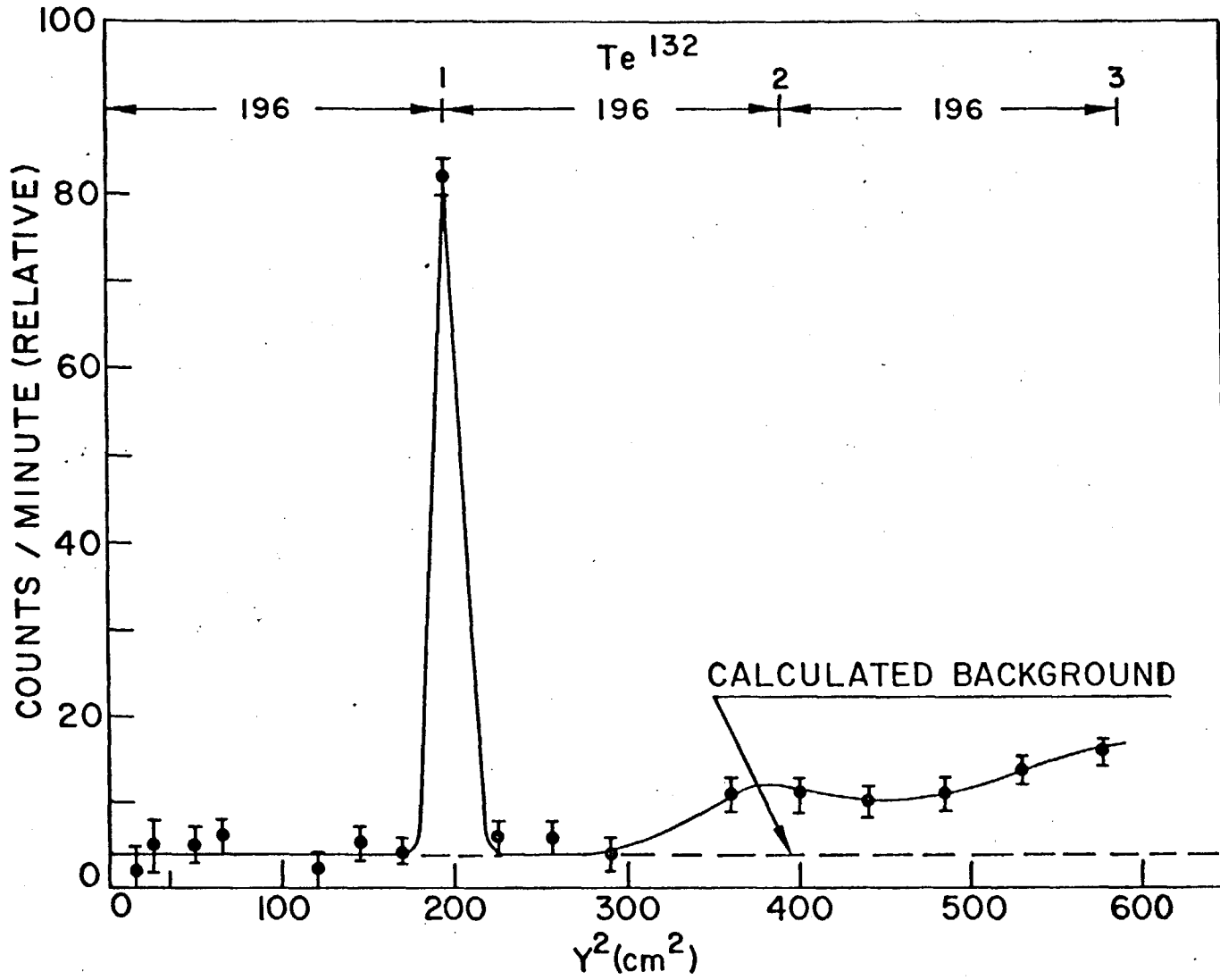


Fig. 13 - UCRL-6491 Rev. 11  
Authors: P.C. Stevenson and  
H.C. Hicks

*PL*

5001859

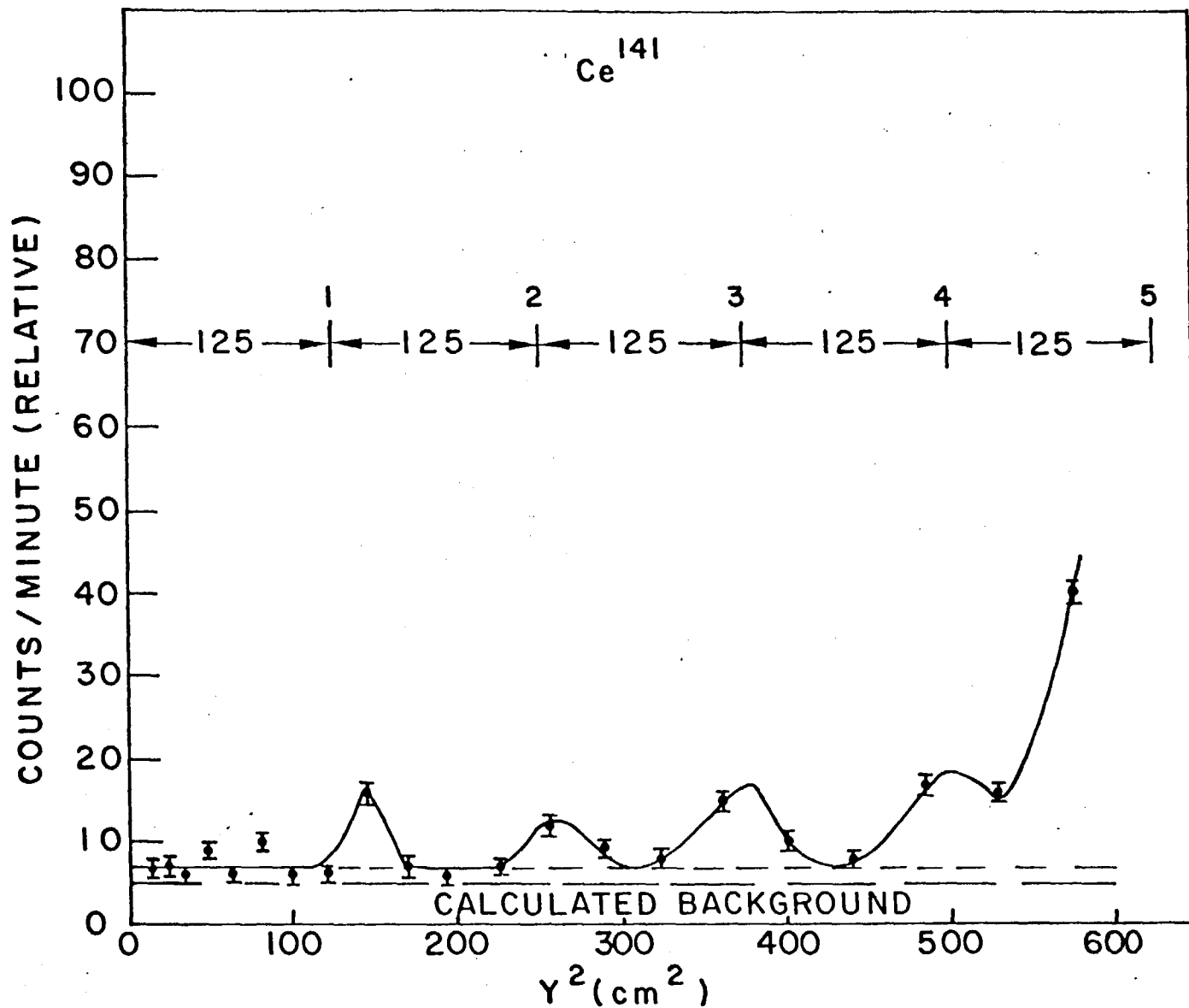


Fig. 14 - UCRL-6491 Rev. II  
Authors: P.C. Stevenson and  
H.C. Hicks

PC

5001005

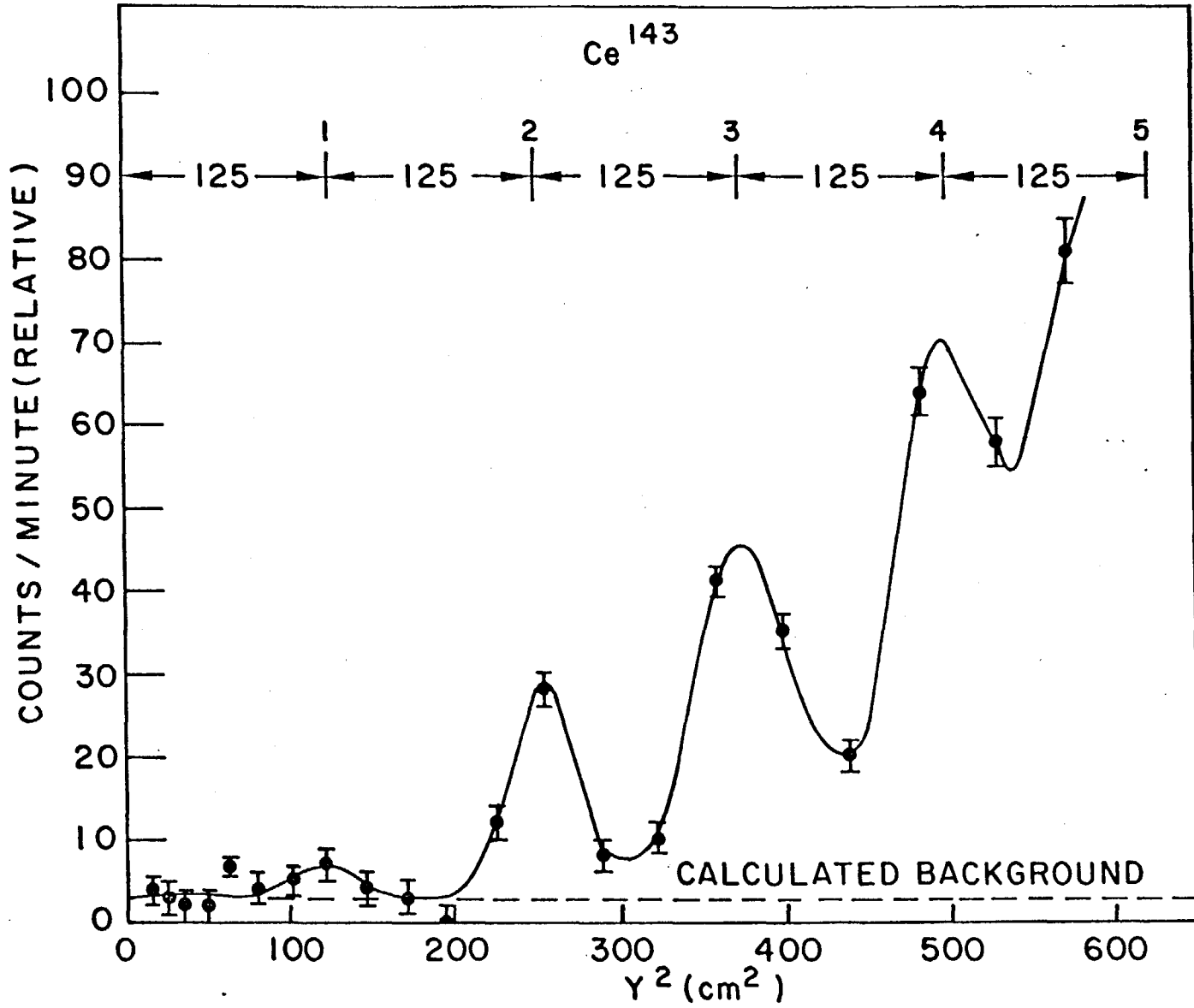


Fig. 15 - UCRL-6491 Rev. II  
Authors: P.C. Stevenson and  
H.C. Hicks

PK

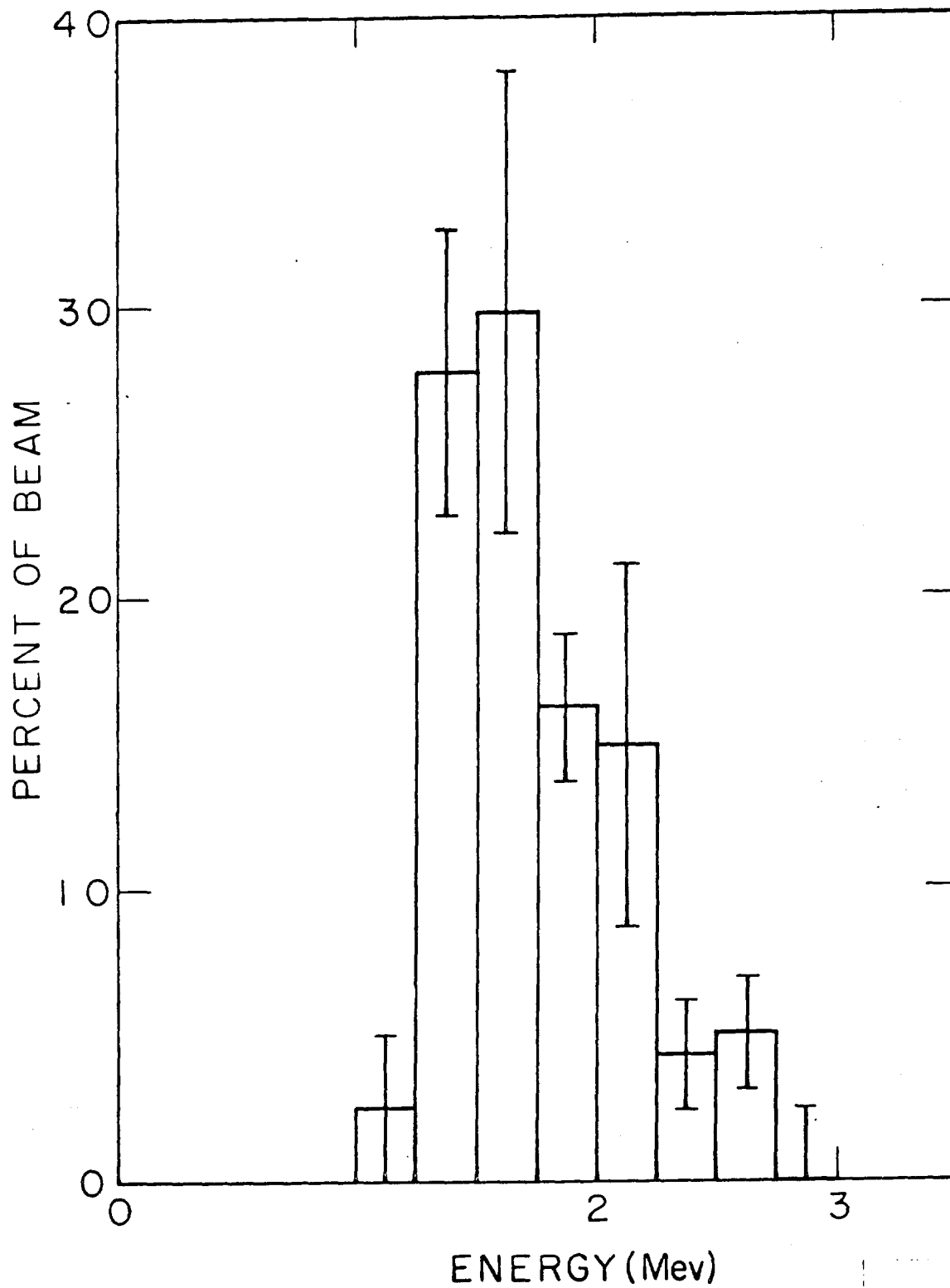


Fig. 16 - UCRL-6491-Rev. II  
 Authors: P. C. Stevenson and  
 H. C. Hicks

5001861

JK